First International Conference on Rail Transportation
Chengdu, China, July 10-12, 2017

Power regeneration in the primary suspension of a railway vehicle

Ruichen Wang, David Crosbee, Simon Iwnicki, Yunshi Zhao and Adam Bevan
Institute of Railway Research, University of Huddersfield, Huddersfield HD1 3DH, UK
**Corresponding author email: r.wang@hud.ac.uk*

Abstract: This paper presents an assessment of the potential for the use of power regenerating devices (PRDs) in railway vehicle primary suspension systems and the evaluation of the potential power that can be obtained. Implications for ride comfort and running safety are also commented on. Several case studies of generic railway vehicle primary suspension systems are modelled and modified to include a power regenerating device. Simulations are then carried out on track with typical irregularities for a generic UK passenger vehicle. The performance of the modified vehicle including regenerated power, ride comfort and running safety is evaluated. Analysis of key influencing factors are also carried out to examine their effects on power capability, ride comfort and running safety to guide the primary suspension design/ specification.
Keywords: railway vehicle, primary damper, power regeneration, ride comfort, running safety

1 Introduction

The possibility of using recoverable energy in vehicle suspension systems has attracted significant attention in recent years. Various design concepts and structures of regenerative suspensions have been proposed and investigated for the recovery of the energy of motion and vibration from road/track disturbances. However, these studies concentrate on the energy conversion from kinetic energy to electricity in road transports (F. Yu et al. 2005; Karnopp 1992; C. Yu et al. 2009; Liang & Shao 2008; Mossberg et al. 2012).

Meanwhile, rail transport (passenger use and Freight use) is equally important in our daily life and also plays an irreplaceable role in the regional economy development. In a typical passenger rail vehicle, much of the energy is wasted by the resistance from track irregularity, friction of moving parts and thermal losses. The kinetic energy loss of the primary and secondary dampers are one of the notable causes of energy losses in rail vehicle, with a total dissipated power ranging from 3.5 to 3.8kW per vehicle (Matamoros-Sanchez 2013).

With theoretical modelling analysis, Zuo and Zhang (Zuo & Zhang 2013) investigated potential energy regeneration in different possible applications, and showed that 5kW-6kW can be recovered from dampers on railway vehicles running on typical tracks (Lei Zuo 2011). Although much of the research into regenerative techniques has been done in road vehicles regarding the potential power and regenerated power, the focus of this work aims toward recovering a considerable power from a vertical primary damper in rail vehicle.

Regenerative techniques in vehicle suspension systems can be classified into three main configurations according to their operating principles: Mechanical, electromagnetic and hydraulic regenerative suspensions (Zhang et al. 2013).

Mechanical: Mechanical regenerative suspension normally uses hydraulic/pneumatic power to convert the kinetic energy into potentially recoverable mechanical energy with control methods, which can be stored for later use (Wendal & Stecklein 1991; Fodor &

Redfield 1992; Jolly & Margolis 1997; Aoyoma et al. 1990; Norisugu 1999; Stansbury 2014).

Electromagnetic (linear/rotary motor): Electromagnetic regenerative suspension converts the relative vibration isolation into the linear or rotary motion using electric generators to produce recoverable electricity (Karnopp 1989; Ryba 1993; Gupta et al. 2003; Zuo et al. 2010; Okada et al. 1998; Suda et al. 1998; Cao et al. 2008; Zheng & Yu 2005; Li et al. 2013; Hayes et al. 2005; Beno et al. 2005).

Hydraulic: Hydraulic regenerative suspension converts the reciprocating linear motion into unidirectional rotary motion through the designed hydraulic circuit, and hence to produce electricity by a generator (Zhang et al. 2015; Fang et al. 2013; Li & Tse 2013; Li et al. 2014; Wang et al. 2016).

To advance power regenerating techniques in railway vehicles, a primary suspension system with efficient power regenerating devices (which is parallel to each primary damper) has been designed and used to characterise the rail vehicle's dynamic response and the power capability with different running speeds, loads, track irregularities and damping coefficient of the primary dampers. These results have been used to evaluate the ride comfort and running safety performance by utilising a PRD. The main objective of this work is to verify the feasibility of the proposed regenerating device in a typical railway application prior to further optimisation and improvement.

2 System modelling

2.1 Rail Vehicle Model

The dynamics of a passenger vehicle is extremely complex with several significant nonlinearities and substantial undefined variables such as the dynamic contact relations in the wheel-rail contact area, the suspension systems and the response of the track. In general, most passenger rail vehicles have a similar basic configuration as shown in Figure 1, which shows a simplified side-view of a half car. The car body is supported by two bogies via the secondary suspension. In each bogie, the wheelsets are connected to the bogie by the primary suspension system (often consisting of passive springs and dampers connected in parallel).

In the modelling system, a PRD has been installed in parallel with each primary vertical damper in a rail car to capture the power and search for optimal electrical damping (additional damping) in the vertical direction. The key parameters of a typical UK passenger vehicle are shown in Table 1.

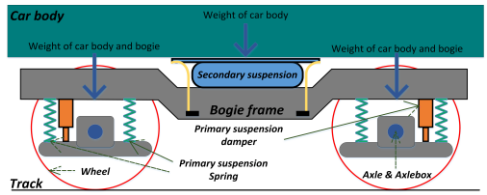

Fig. 1 Simplified side-view of a rail vehicle

Table 1 Values of parameters of a typical passenger rail vehicle.

Symbol	*Definition*	*Value*
m_{veh}	Total vehicle mass	33,000kg
m_{bd}	Car body mass	25,080kg
m_{bg}	Total bogie frame mass (Include 8 proposed PRD; 2.5kg each)	4,180kg
m_{ws}	Per wheelset mass	1,120kg
k_{sv}	Secondary vertical stiffness (Per axlebox)	1.368×10^5N/m
c_{sv}	Secondary vertical damping (per damper)	1.337×10^4Ns/m
k_{pv}	Primary vertical stiffness (Per axlebox)	7.599×10^5N/m
c_{pv}	Primary vertical damping (per damper)	3,800Ns/m
B_{wb}	Bogie wheelbase	2.6m
C_h	Body height	1.57m
B_h	Bogie height	0.5m
W_r	Wheel radius	0.45m
H_{pvt}	Primary vertical damper height (top)	0.81m
H_{pvb}	Primary vertical damper height (bottom)	0.29m
L_{hl}	Half body length	12m
L_{hw}	Half body width	1.4m

Based on the defined typical passenger vehicle model and track data, Figure 2 illustrates the modelling procedure and performance evaluation including track roughness, dynamic rail vehicle model and rail vehicle response variables in the time domain. The dynamic performance is simulated using the commercial software VAMPIRE (Resonate 2016) under various driving speeds and track irregularities and the outputs include primary suspension vertical velocity, wheel-rail contact forces (lateral force and vertical force), weighted RMS accelerations of body centre, pivot1 and pivot2 (in longitudinal, lateral and vertical directions), damping force, potential power and regenerated power.

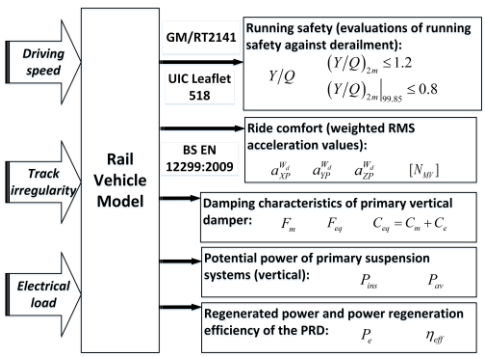

Fig. 2 Block diagram view of overall rail vehicle dynamics

2.2 Track Irregularity

Normally, the track inputs can be divided in to two types: predefined inputs and random inputs. First, the track data is mostly defined as a variety of well-defined track design features (gradients, curves and cant deficiency, etc). Then the irregularity of the track can be characterised by the vertical and lateral displacements of the rail from the design alignment. The roughness of track can be characterised by a power spectrum to express the track irregularities and imperfections based on different defined standards, or based on measured data from real tracks. As a basis for comparison, the predefined track using a sinusoidal irregularity with a given frequency and amplitude is insufficient for investigating the performance of a given suspension system or damper system, so real measured track data is considered in this study.

The track surface roughness is the key source of track-induced vibration for a railway vehicle. Several studies of the regenerative dampers have carried out with simulations using well-defined track inputs which are regard to a stochastic modelling of the track geometry. In order to accurately quantify the potential power, ride quality and running safety, measured track inputs will be used in this study. Therefore, data from three different tracks as shown in Table 2 are applied into the rail vehicle simulations as track inputs.

Table 2 General track data characteristics and descriptions (Resonate 2016).

Track	*Line Speed*	*Length*	*Std. Dev. (Lateral)*	*Std. Dev. (Vertical)*
Track 110	177 km/h	5km	3.04mm	5.12mm
Track 200	321.9 km/h	5km	1.42mm	2.39mm
Track 270	434.5 km/h	4km	1.04mm	1.81mm

Track	*Description*
Track 110	A low speed, 110km/h (70mph) piece of UK track, lower quality cross country track
Track 200	A good quality piece of UK mainline track, 200km/h(125mph), typical of high speed intercity track
Track 270	Top quality German ICE track, 270km/h (170mph)

2.3 Power Regenerating Device

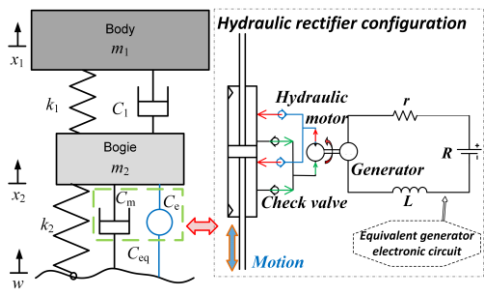

Fig. 3 Simplified diagram of the suspension systems and PRD (Wang 2016)

Considering the cost, efficiency and reliability, a hydraulic rectifier configuration has the most potential for meeting the demands of the development trend of future rail vehicle dampers. As shown in Figure 4, a schematic design of a PRD is proposed which consist of a

double acting hydraulic cylinder, a hydraulic rectifier (four check valve arrangement), a hydraulic motor, and a generator.

The hydraulic cylinder is designed to have four ports, which are distributed at both sides of the cylinder body, four check valves have been connected which act as a hydraulic rectifier. Through rectification, the hydraulic fluid during the bounce and rebound motions pass through the hydraulic motor in one direction. The hydraulic motor is directly coupled to the generator, and driven by the pressurised flow. The hydraulic motor converts the linear motion of the primary suspension system into rotary motion by fluid transfer, and then the succeeding rotation of the hydraulic motor drives the generator to generate electricity (Wang et al. 2016).

Table 3 Values of key parameters of the PRD (Wang et al. 2016).

Symbol	*Value*	*Unit*
A_m *(Radius)*	1.27×10^{-4} (6.35)	m^2 (mm)
D_m	8.2	cc ($\times10^{-6}$ m^3)
k_T	0.925	Nm/A
k_V	0.925	V/(rad/s)
η_v	92	%
η_m	95	%
r	10	Ω
R	20	Ω

Figure 3 shows a simplified primary suspension system using a hydraulic PRD which can be executed with the standard fluid viscous damper in parallel. It can be noted that the PRD can provide desirable damping by adjusting electrical load R to reach an appreciate damping whilst recovering power for energy saving.

Using a PRD, energy from the track roughness induced vibrations can be converted into recoverable energy which can be stored in a battery/cell for further use, and an appropriate damping rate can be provided by adjusting the electrical load which can be further developed for semi-active control or self-powered force control.

Based on a typical passenger rail vehicle model, PRD and measured track data, an evaluation criteria for ride comfort, running safety, potential power and regenerated power, which can be met by primary suspension system, is presented. The evaluation is dependent on the average power, power efficiency, wheel-rail contact forces and accelerations of car body and bogies. This study is intended to give a design guideline for the use of a regenerative primary damper; the primary damper in a rail vehicle is not only for power generation, but also the dynamic performance in terms of running safety and passenger comfort.

In the proposed system, the equivalent damping of primary damper and PRD can be written as (Fang & Guo 2013):

$$C_{eq} = C_m + C_e \tag{1}$$

where C_{eq} is the equivalent damping coefficient of the primary damper, C_m is the viscous damping coefficient, C_e is the electric damping coefficient, respectively. The electric damping coefficient is (Fang & Guo 2013):

$$C_e = \left(\frac{2\pi A_m}{D_m}\right)^2 \left(\frac{k_T k_V}{r+R}\right)\frac{\eta_v}{\eta_m} \tag{2}$$

where A_m is the area of hydraulic cylinder cross-sectional area, D_m is the displacement of the hydraulic motor, k_T is the torque constant coefficient, k_V is electromotive voltage constant coefficient, r is the internal resistance of the generator, R is the external load, η_v and η_m are the volumetric and mechanical efficiency of the hydraulic motor. The hydraulic motor flow rate is given by:

$$Q_m = A_m \cdot v \tag{3}$$

where v is the vertical velocity of the primary damper. The motor/generator shaft speed can be calculated by:

$$\omega_m = \frac{2\pi Q_m \eta_v}{D_m} \tag{4}$$

The generator used in the PRD should be mechanically simple for ease of functionality and operability. Therefore, an equivalent DC permanent magnetic generator has been

modelled and embedded into the primary suspension system in this study. Electromotive force (EMF) is highly dependent on the generator armature speed and field current.

The electromotive force (EMF) E and the instantaneous electrical current I are given by (Eremia & Shahidehpour 2013):

$$E = k_V \cdot \omega_m \quad \text{and} \quad I = \frac{E}{R + r} \tag{5}$$

and regenerated power is the power that recovered by the PRD for reuse, which can be calculated as:

$$P_e = I^2 \cdot R \tag{6}$$

Generally, the primary suspension velocity is representative of the vertical velocity between wheelsets and bogies, and has a significant effect on power dissipation of a damper. However, it can be determined that the potential power is the maximum recovery of the power dissipation by primary damper. Therefore, the instantaneous potential power can be simplified as follows:

$$P_{ins} = c_{eq} \cdot v^2 \tag{7}$$

and the average potential power is:

$$P_{av} = \frac{1}{T}\int_0^T C_{eq} \cdot v^2 dt \tag{8}$$

where T is the time end and dt is the time interval. Table 3 shows the model-related component parameters of the PRD such as the hydraulic rectifier and generator specifications. And the power regeneration efficiency is given by:

$$\eta_{eff} = \frac{P_e}{P_{av}} \tag{9}$$

Equation (2) represents the damping coefficient of the PRD and shows that damping is dependent on electrical load. According to Equation (2), it indicates that the damping coefficient can be adjusted in a large range by controlling the external electrical load or specific charge circuit. In such a prediction, the electrical damping is decreased with the increase of the electrical load.

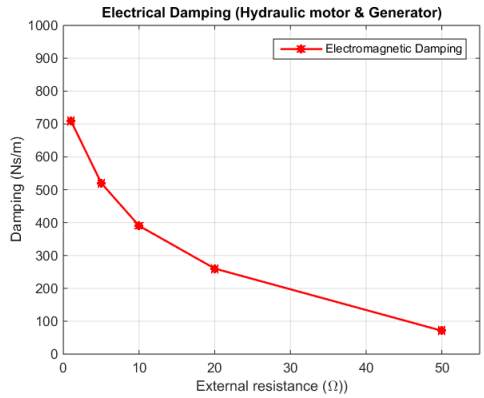

Fig. 4 Electrical damping coefficient with different electrical loads

Figure 4 shows that electrical damping can act as additional damping when applied to the primary suspension system. This allows adjustment of the damping whilst recovering power for energy saving. A 1Ω electrical load can provide a damping coefficient of around 710 Ns/m, which is approximate to 1/6 of the viscous damping of existing primary damper whilst a larger electrical load over 50Ω offers less additional damping coefficient, which approaches to zero.

2.4 Ride Comfort

The suspension system of modern passenger rail vehicles ensure the ride quality for the passengers and staff over different track irregularities. The suspension system acts as a key component to suppress the track-induced vibration therefore its dynamic performance has a significant influence on the ride quality.

The accelerations of ride comfort in accordance with the statistical method can be calculated by:

$$a_{XP}^{W_d}(t) = \left[\frac{1}{T} \cdot \int_{t-T}^{t} (\ddot{x}_{W_d}^{*}(\tau))^2 d\tau\right]^{0.5} \tag{10}$$

where a is root mean square (RMS) value of acceleration (>5s), W_d is the weighted frequency value in accordance with x-axis (x-longitudinal direction), P is the floor interface, T is equal to 5s and t is a multiple of 5s.

$$a_{YP}^{W_d}(t)=\left[\frac{1}{T}\cdot\int_{t-T}^{t}(\ddot{y}_{W_d}^{*}(\tau))^2 d\tau\right]^{0.5} \quad (11)$$

where W_d is the weighted frequency value in accordance with Y-axis (y-lateral direction)

$$a_{ZP}^{W_b}(t)=\left[\frac{1}{T}\cdot\int_{t-T}^{t}(\ddot{z}_{W_b}^{*}(\tau))^2 d\tau\right]^{0.5} \quad (12)$$

where W_b is the weighted frequency value in accordance with Z-axis (z-vertical direction)

According to the BS EN 12299-2009 standard of ride comfort−railway applications (BS EN12299, 2009), the 95th percentiles of the distributions of five-second weighted RMS-values calculated over a time period of 5 mins are denoted as $a_{XP95}^{W_d}$, $a_{YP95}^{W_d}$ and $a_{ZP95}^{W_b}$. Hence, the partial comfort indexes (longitudinal, lateral and vertical) can be expressed as:

$$\begin{aligned} N_{MVx}&=6\cdot a_{XP95}^{W_d}\\ N_{MVy}&=6\cdot a_{YP95}^{W_d}\\ N_{MVz}&=6\cdot a_{ZP95}^{W_b}\end{aligned} \quad (13)$$

Hence, the ride comfort indices N_{MV} according to the statistical method can be calculated by means of Equations (1)-(3):

$$N_{MV}=6\cdot\sqrt{(a_{XP95}^{W_d})^2+(a_{YP95}^{W_d})^2+(a_{ZP95}^{W_b})^2} \quad (14)$$

According to the particular interest of the ride comfort indices N_{MV}, the standard of ride comfort indications defined in Table 4 to provide an obvious criterion:

Table 4 N_{MV} evaluation scales – ride comfort (BS EN12299, 2009).

Scale for the N_{MV} Comfort Index	
N_{MV} <1.5	Very comfortable
1.5≤ N_{MV} ≤2.5	Comfortable
2.5≤ N_{MV} ≤3.5	Medium
3.5≤ N_{MV} ≤4.5	Uncomfortable
N_{MV} ≥4.5	Very uncomfortable

2.5 Running Safety

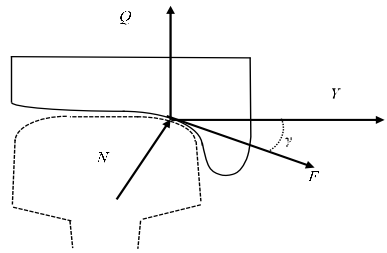

Fig. 5 Wheel-rail contact forces: *Y* (lateral force), *Q* (vertical force), *N* (normal force) and *F* (lateral rolling friction force).

Running safety is determined by the wheel-rail contact forces (lateral and vertical) which are exchanged between the wheel and the rail. One of the main risks of derailment is realised when a there is large lateral force and a low vertical force acting between the wheel and the rail allowing the wheel flange to climb up the rail gauge face rapidly resulting in a derailment. Therefore, the safety requirements on the wheel-rail contact performance of rail vehicle needs are considered as a key performance.

The wheel-rail contact force ratio can be calculated in term of the lateral force and vertical force at various driving speeds and different electrical loads. Based on the Nadal criterion (Nadal 1896) and GM/RT2141 (RSSB 2009) which shall nowhere exceed 1.2, it can be shown as follows:

$$\frac{Y}{Q}<\frac{\tan\alpha-\mu}{1+\mu\tan\alpha},\ (Y/Q)_{2m}\le 1.2 \quad (15)$$

where μ is the friction coefficient at the contact point and α is the maximum flange contact angle.

$$(Y/Q)_{2m}\big|_{99.85}\le 0.8 \quad (16)$$

where *2m* is the running average at each 2 metres track point (*1m* forward and back), $(Y/Q)_{2m}\big|_{99.85}$ is the 99.85 percentile value which is limited by 0.8 (UIC Leaflet 518 2009).

3 Analysis, Results and Discussion

To evaluate the ride comfort, running safety, potential power and regenerated power, the rail vehicle primary suspension system developed in Section 2.3 was used with different vehicle running speeds and electrical loads.

3.1 Ride Comfort and Running Safety

In order to assess the comparative ride performance under different operating conditions, simulations were undertaken at constant speed using approximately of 30km of measured track geometry selected to be representative of the track seen by the modelled passenger rail vehicle. The simulation conditions can be summarised as follows:

- *Vehicle type:* a generic 33t passenger vehicle
- *Wheel-rail contact:* New P8 wheel, new 56E1 rail
- *Track cases:* ≈30km measured track geometry
- *Wheel-rail Friction coefficient:* 0.32
- *Running speeds:* 25, 50, 75, 100, 125mph (with 1Ω electrical load) (40.2, 80.5, 120.7, 160.9, 201.2km/h)
- *Electrical loads:* 1, 5, 10, 20, 50Ω (at 100mph vehicle running speed)

Accelerations were predicted on the vehicle body at floor level above the leading and trailing bogie pivots and at the body centre. These were the weighted according to the lateral (W_d) and vertical (W_b) passenger comfort filters contained in Euro-Norm EN 12299:2009 (BS EN12299, 2009). The mean ride comfort of body centre, pivot 1 and pivot 2 were calculated with different running speeds and electrical loads which is shown in Table 5.

The mean ride comfort is generally worse with the increase of the vehicle running speed at body centre, pivot 1 and pivot 2. In the worst case (100mph), the mean ride comfort N_{MV} at pivot 2 are up to 2.2 but it is still fairly comfortable for the human vibration sensitivity. In addition, it confirms that the ride performance is not tied on the electrical load in electric circuit of primary suspensions but it highly depends on secondary suspensions.

Table 5 Ride comfort assessment under different vehicle speeds and external loads.

95th Percentile Weighted RMS Acceleration (Mean Ride comfort)			
Running Speed (Load: 1Ω):	*Body Centre*	*Pivot 1*	*Pivot 2*
25mph(40.2km/h)	0.58	0.73	0.83
50mph(80.5km/h)	0.65	1.25	0.98
75mph(120.7km/h)	0.75	1.24	1.37
100mph(201.2km/h)	1.17	1.80	2.20
Load Resistance (Speed: 100mph [160.9km/h]):	*Body Centre*	*Pivot 1*	*Pivot 2*
1Ω	1.17	1.80	2.20
5Ω	1.17	1.80	2.20
10Ω	1.17	1.80	2.20
20Ω	1.18	1.79	2.20
50Ω	1.17	1.80	2.20

Next, simulations were carried out to examine the resistance of the proposed vehicle model to low speed flange climbing derailment according to requirements of GM/RT2141 (RSSB 2009) and UIC Leaflet 518 (UIC Leaflet 518 2009). The following conditions were considered:

- *Wheel-rail friction coefficient:* 0.32
- *Running speed:* Trundle (2m/s)
- *Track cases:* see the following Table:

Radius (m)	*Cant (mm)*	*Gauge Widening (mm)*	*Transition Length (m)*
90	25	19	7.5
150	100	13	30
200	150	6	45

Table 6 shows the ratio of lateral to vertical force (Y/Q) for the leading wheest outer wheel using different curve radii at 1Ω. In all case predicted Y/Q remains below both the Nadal limit of 1.2 and the 99.85 percentile limit of 0.8. Therefore, based on the results of the Weighted RMS acceleration and Y/Q, it can be summarised that the applied PRD has a slight influence on ride comfort and running safety but the ride comfort and running safety are higly

reliant on the vehicle running speed and track irregualrity.

Table 6 Y/Q low speed flange climb case at 1Ω electrical load.

Radius	*Transition**	*Maximum Y/Q (<1.2)*	*Max 99.85th Percentiles (<0.8)*
90	Bottom	0.904	0.715
90	Top	0.856	0.699
150	Bottom	0.830	0.605
150	Top	0.940	0.760
200	Bottom	1.051	0.720
200	Top	0.908	0.677

*Distance from start of run-off transition to centre of dip

3.2 Effect of Running Speed

Firstly, vehicle running speeds are modelled as the first influencing factor on power capability and damping characteristic. In Figure 6 and 7, it is clear that the average EMF and the peak value of force-velocity loop increase with various vehicle running speeds ranging from 25mph (40.23km/h) to 125mph (201.2km/h). It can be summarised that vehicle speed is the key factor for the capability of power regeneration in proposed primary suspension system, and the running speed will be considered to develop the design and the practical use of a power regenerative device.

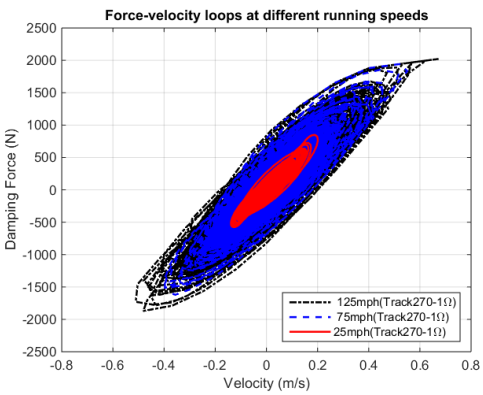

Fig. 6 Equivalent damping force at different vehicle running speeds

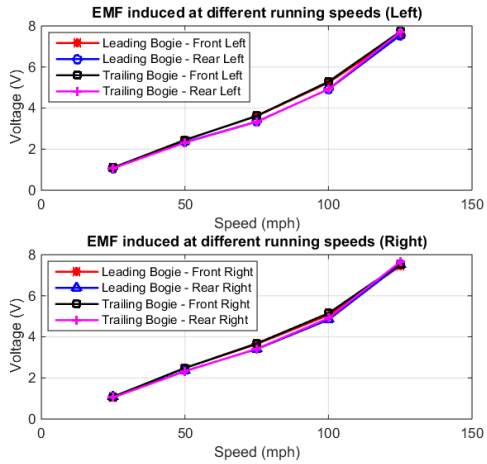

Fig. 7 Average electromotive force (EMF) of a car (8 primary dampers, 4-left and 4-right) at various vehicle running speeds

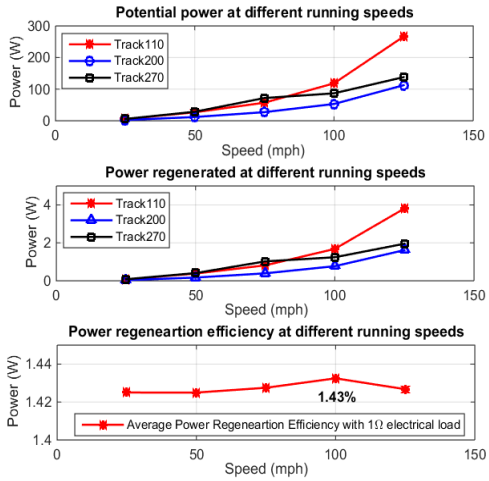

Fig. 8 Potential power, Power regenerated and average power regeneration efficiency of a car at various vehicle running speeds

Figure 8 shows that the average of the potential power and regenerated power are predicted at different measured tracks with the vehicle running speed increased from 25mph (40.23km/h) to 125mph (201.2km/h) gradually. The power in values are mildly increased with the incident speeds, and the faster running speed can produce more excitation events and thus to provide more potential power and regenerated power but the power regeneration efficiencies have no obvious increases which are 1.425%,

1.425%, 1.428%, 1.43% and 1.427%, respectively.

At a running speed of 125mph (201.2km/h), there is a range of potential power from 112.3W to 266.2W for all primary dampers of a car when a rail vehicle runs on typical 'track110', 'track200' and 'track270'. It clearly shows that the regenerated power in primary suspension systems has a great potential to recharge the electronic equipment of vehicle.

3.3 Effect of Electrical Load

The following analysis will explore the characteristics of the potential power, regenerated power and damping force at various electrical loads. With the damping recalculation in Section 2.3, the equivalent damping coefficient of the primary damper can be found in Figure 9, and the predicted results show the trend of damping coefficient and damping force which are degraded with the growth of the load resistance. As shown in Figure 9(b) and (c), the peak values of the damping force are occurred at 1Ω electrical load, which is around 435N in all primary dampers of a car.

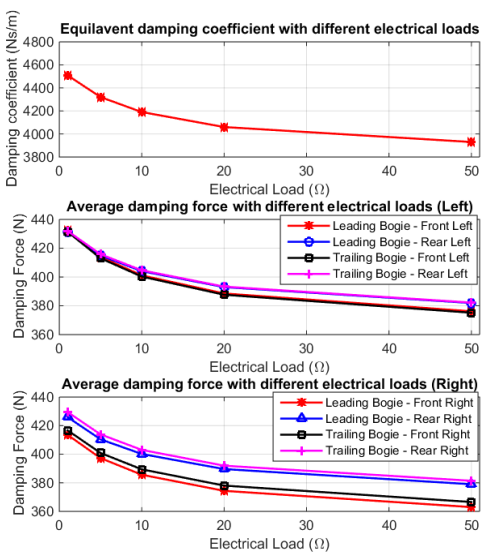

Fig. 9 Equivalent damping coefficient and damping forces analysis of a car with different electrical loads

In Figure 10(a), the increase of the electrical load has no significant effect on the potential power of the primary damper. As shown in Figure 10(b), the peaks of power can be regenerated using the load resistance of 10Ω in each of running condition (track-speed). In addition, a maximum of 4.66% power regeneration efficiency can be also achieved at a 10Ω, which is identical to the internal resistance of the generator.

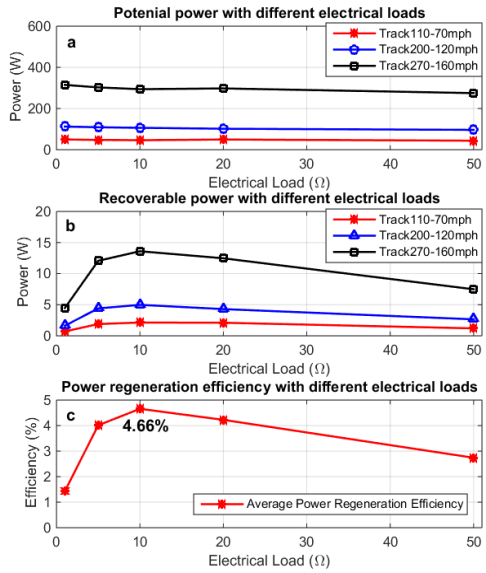

Fig. 10 Power potential, regeneration and average power regeneration efficiency of a car with different electrical loads

Figure 10(a) and (b) indicate that the optimal power regeneration with maximum regenerating efficiency can be reached through the impedance matching.

4. Conclusions

In this paper, the potential power and regenerated power of the rail vehicle primary suspensions induced by track irregularities have been evaluated and the influence that such a system will have on the performance of ride quality and running safety has been investigated. The results show that **(A)** the equivalent damping coefficient depends on the electrical loads. **(B)** A potential power output of 5-270W is available from the primary damper of a typical passenger rail vehicle at 125mph (201.2km/h) on a poorer quality low speed track. **(C)** The applied external electrical load in the PRD has no significant effect on ride comfort and running

safety of a rail vehicle. **(D)** As a result, with improvement of regenerative suspension techniques, the PRD has a great potential to replace the conventional primary damper.

References

Aoyoma, Y. et al., 1990. Development of the Full Active Suspension by Nissan. SAE Technical Paper 901747.

Beno, J.H., Worthington, M.T. & Mock, J.R., 2005. Suspension Trade Studies for Hybrid Electric Combat Vehicles. SAE Technical Paper 2005-01-0929.

BS EN12299, 2009. Railway applications - ride comfort for passengers – measurement and evaluation.

Cao, M., Liu, W. & Yu, F., 2008. Development on electromotor actuator for active suspension of vehicle. Chinese Journal of Mechanical Engineering, 44(11), pp.224–228.

C. Yu, W. Wang & Q. Wang, 2009. Analysis of energy-saving potential of energy regenerative suspension system on hybrid vehicle. Journal of Jilin University, 39(4), pp.841–845.

Eremia, M. & Shahidehpour, M., 2013. Handbook of Electrical Power System Dynamics: Modelling, Stability, and Control, John Wiley & Sons.

Fang, Z. et al., 2013. Experimental study of damping and energy regeneration characteristics of a hydraulic electromagnetic shock absorber. Advances in Mechanical Engineering, 5, p.943528.

Fang & Guo, 2013. An optimal algorithm for energy recovery of hydraulic electromagnetic energy-regenerative shock absorber. Applied Mathematic & Information Sciences, 7(6), pp.2207–2214.

F. Yu, M. Cao & X. C. Zheng, 2005. Research on the feasibility of vehicle active suspension with energy regeneration. Journal of Vibration and Shock, 24(4), pp.27–30.

Fodor, M.G. & Redfield, R.C., 1992. The variable linear transmission for regenerative damping in vehicle suspension control. In American Control Conference, 1992. American Control Conference, 1992. pp. 26–30.

Gupta, A., Mulcahy, T.M. & Hull, J.R., 2003. Electromagnetic shock absorbers. In Proceedings of the 21th Model Analysis Conference : Conference & Exposition on Structural Dynamics.

Hayes, R.J., Beno, J.H. & Weeks, D.A., 2005. Design and testing of an active suspension system for a 2-1/2 ton military truck. SAE Technical Paper 2005-01-1715.

Jolly, M.R. & Margolis, D.L., 1997. Regenerative systems for vibration control. Journal of Vibration and Acoustics, 119(2), pp.208–215.

Karnopp, D., 1989. Permanent magnet linear motors used as variable mechanical dampers for vehicle suspensions. Vehicle System Dynamics, 18(4), pp.187–200.

Karnopp, D., 1992. Power requirements for vehicle suspension systems. Vehicle System Dynamics, 21(1), pp.65–71.

Lei Zuo, 2011. Energy Harvesting Shock Absorbers. In Premier Conference for Advanced Energy. New York.

Li, C. et al., 2014. Integration of shock absorption and energy harvesting using a hydraulic rectifier. Journal of Sound and Vibration, 333(17), pp.3904–3916.

Li, C. & Tse, P.W., 2013. Fabrication and testing of an energy-harvesting hydraulic damper. Smart Materials and Structures, 22(6), p.65024.

Li, Z. et al., 2013. Electromagnetic energy-harvesting shock absorbers: Design, Modelling, and Road Tests. IEEE Transactions on Vehicular Technology, 62(3), pp.1065–1074.

Liang, J. & Shao, C., 2008. Research on an energy-regenerative active suspension for vehicles. Vehicle & Power Technology, 17(1).

Matamoros-Sanchez, A.Z., 2013. The use of novel mechanical devices for enhancing the performance of railway vehicles. Thesis. © Alejandra Z. Matamoros-Sanchez.

Mossberg, J. et al., 2012. Recovering Energy from Shock Absorber Motion on Heavy Duty Commercial Vehicles. SAE Technical Paper 2012-01-0814.

Nadal, J., 1896. Theorie de la Stabilite des locomotives, Part II: mouvement de lacet, Annales des Mines.

Norisugu, T., 1999. Energy saving of a pneumatic system (2). Energy regenerative control of a pneumatic drive system. Journal of Application to Active Air Suspension, Hydraulics & Pneumatics, 38(4), pp.1–4.

Okada, Y., Yonemura, J. & Shibata, M., 1998. Regenerative control of moving mass type vibration damper. Proceedings of the 4th International Conference on Motion and Vibration Control (MOVIC), Zurich, Switzerland, pp.85–90.

Resonate, 2016. VAMPIRE® | Home. Available at: http://www.vampire-dynamics.com/.

RSSB, 2009. Railway Group Standard GM/RT2141: Resistance of railway vehicles to derailment and roll-over,

Ryba, D., 1993. Semi-active damping with an electromagnetic force generator. Vehicle System Dynamics, 22(2), pp.79–95.

Stansbury, J., 2014. Regenerative suspension with accumulator systems and methods.

Suda, Y., Nakadai, S. & Nakano, K., 1998. Study on the self-powered active vibration control.

In Proceedings of the 4th International Conference on Motion and Vibration Control.

UIC Leaflet 518, 2009. Testing and approval of railway vehicles from the point of view of their dynamic behaviour-Safety-Track fatigue-Ride quality, Railway Technical Publications.

Wang, R. et al., 2016. Modelling, Testing and Analysis of a Regenerative Hydraulic Shock Absorber System. Energies, 9(5), p.386.

Wang, R., 2016. Modelling, testing and analysis of a regenerative hydraulic shock absorber system. Huddersfield, UK: University of Huddersfield.

Wendal, G. & Stecklein, G., 1991. A Regenerative Active Suspension System. SAE Publication SP-861, Paper No. 910659, pp.129–135.

Zhang, J. et al., 2013. A review on energy-regenerative suspension systems for vehicles. In Proceedings of the World Congress on Engineering. London, UK, pp. 1889–1892.

Zhang, Y. et al., 2015. Study on a novel hydraulic pumping regenerative suspension for vehicles. Journal of the Franklin Institute, 352(2), pp.485–499.

Zheng, X. & Yu, F., 2005. Study on the potential benefits of an energy-regenerative active suspension for vehicles. SAE transactions, 114(2), pp.242–245.

Zuo, L. et al., 2010. Design and characterization of an electromagnetic energy harvester for vehicle suspensions. Smart Materials and Structures, 19(4), p.45003.

Zuo, L. & Zhang, P.-S., 2013. Energy harvesting, ride comfort, and road handling of regenerative vehicle suspensions. Journal of Vibration and Acoustics, 135(1), p.11002.